Report

Cell Reports

Joint Development Involves a Continuous Influx of Gdf5-Positive Cells

Graphical Abstract

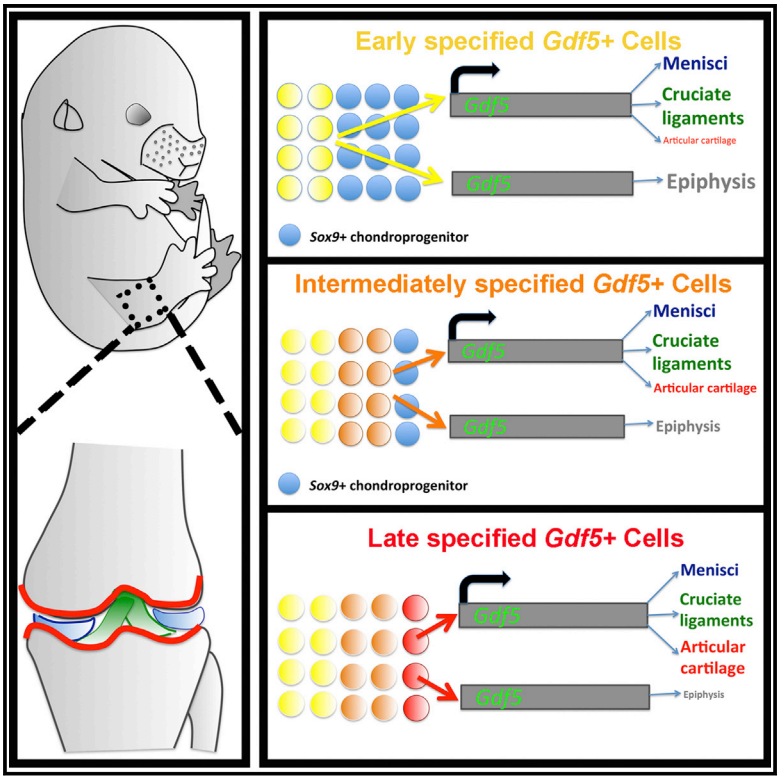

Highlights

- Synovial joint development involves a continuous influx of cells into the interzone
- *Gdf5*-positive interzone cells contribute differentially to various joint tissues
- The complex spatiotemporal dynamics of *Gdf5* expression may instruct lineage divergence
- The influx model expands the current view of joint development

Authors

Yulia Shwartz, Sergey Viukov, Sharon Krief, Elazar Zelzer

Correspondence

eli.zelzer@weizmann.ac.il

In Brief

Synovial joints are assumed to originate from a set of early-specified progenitors. Using a knockin *Gdf5-CreER*^{T2} mouse, Shwartz et al. show that joints develop through a continuous influx of cells into the interzone. The complex spatiotemporal dynamics of *Gdf5* expression may reveal a mechanism of lineage divergence.

Shwartz et al., 2016, Cell Reports *15*, 2577–2587
June 21, 2016
http://dx.doi.org/10.1016/j.celrep.2016.05.055

Cell Reports
Report

Joint Development Involves a Continuous Influx of Gdf5-Positive Cells

Yulia Shwartz,[1] Sergey Viukov,[1] Sharon Krief,[1] and Elazar Zelzer[1,*]
[1]Department of Molecular Genetics, Weizmann Institute of Science, Rehovot 76100, Israel
*Correspondence: eli.zelzer@weizmann.ac.il
http://dx.doi.org/10.1016/j.celrep.2016.05.055

SUMMARY

Synovial joints comprise several tissue types, including articular cartilage, the capsule, and ligaments. All of these compartments are commonly assumed to originate from an early set of *Gdf5*-expressing progenitors populating the interzone domain. Here, we provide evidence that joints develop through a continuous influx of cells into the interzone, where they contribute differentially to forming joint tissues. Using a knockin *Gdf5-CreER*^{T2} mouse, we show that early labeling of *Gdf5*-positive interzone cells failed to mark the entire organ. Conversely, multiple Cre activation steps indicated a contribution of these cells to various joint compartments later in development. Spatiotemporal differences between *Gdf5* and *tdTomato* reporter expression support the notion of a continuous recruitment process. Finally, differential contribution of *Gdf5*-positive cells to various tissues suggests that the spatiotemporal dynamics of *Gdf5* expression may instruct lineage divergence. This work supports the influx model of joint development, which may apply to other organogenic processes.

INTRODUCTION

According to the prevailing model, organogenesis is initiated with the specification of a subset of cells as progenitors that are then organized to form a primordium. As development proceeds, the primordium undergoes extensive growth, differentiation, and morphogenesis until the organ obtains its final form (Biehs et al., 2013; Garrison et al., 2009; Göttgens, 2013; Gu et al., 2002; Little, 2011; Stanger et al., 2007; Wilkinson and Göttgens, 2013). Synovial joints are structures that separate adjacent skeletal elements and thus allow locomotion. The mature joint is composed of articular cartilage, synovial fluid, ligaments, and a fibrous capsule, which together function to transmit biomechanical loads during skeletal motion (Decker et al., 2014).

The first histological indication for joint formation is the appearance of a higher cell density domain called the interzone at the site of the future joint. The interzone consists of three layers, the middle of which is termed the intermediate zone (Mitrovic, 1977). Molecularly, interzone cells lose the expression of chondrocyte-specific genes such as collagen type II. Instead, they express a new set of genes that includes growth and differentiation factor 5 (*Gdf5*), *Wnt4*, and *Wnt9a* (Guo et al., 2004; Hartmann and Tabin, 2001; Später et al., 2006; Storm et al., 1994).

Over the years, it has been suggested that interzone cells serve as joint progenitors. Removal of the interzone was shown to lead to joint loss and bone fusion (Holder, 1977). Light and electron microscopy studies have suggested that interzone cells from the two outside layers contribute secondarily to the adjacent epiphyses, whereas intermediate zone cells form the external layers of the joint (Ito and Kida, 2000). Finally, lineage studies utilizing *Gdf5-Cre* mice showed that cells of all mature joint components originate from *Gdf5*-expressing lineages, further promoting the view that interzone cells are joint progenitors (Koyama et al., 2007, 2008; Rountree et al., 2004).

These works support a model in which, during the initial stages of skeletogenesis, a subset of mesenchymal cells is specified as interzone cells to serve as joint progenitors. However, evidence accumulated in recent years indicates that, during development, cells from the vicinity are integrated into the forming joint (Hyde et al., 2008; Koyama et al., 2007; Pacifici et al., 2006; Ray et al., 2015). These findings suggest a more elaborate mode of development, reopening the question of whether joint development follows the widely accepted scheme of organogenesis. In this study, we use a new *Gdf5-CreER*^{T2} knockin mouse line to propose a revised model for joint development. We show that joint development occurs through a continuous influx of new cells that are integrated into the interzone, where they contribute to the forming joint, hence the term influx model. Finally, we show that this mechanism facilitates lineage divergence and, thereby, joint development.

RESULTS

Establishment of the *Gdf5-CreER* Knockin Mouse as a Model System

The current consensus that *Gdf5*-positive interzone cells are joint progenitors has been based on lineage tracing experiments using a *Gdf5-Cre* transgenic mouse. This line was produced by integrating the Cre recombinase sequence into a 140-kb bacterial artificial chromosome (BAC) containing the *Gdf5* locus (Rountree et al., 2004). This transgene might not contain all

of the potential regulatory elements that control endogenous *Gdf5* expression and might also be influenced by the genomic integration site. Therefore, to directly test that view, we sought to generate a *Gdf5-CreER* mouse that would allow us to temporally label *Gdf5*-expressing cells. Taking a knockin approach, we inserted a cassette encoding for *CreER* into the translation start site of the *Gdf5* gene using homologous recombination (Figure S1Aa). To demonstrate both the accuracy and the efficiency of the new *Gdf5-CreER* line, we crossed this mouse with a *Rosa26-tdTomato* reporter line and induced recombination by a single tamoxifen dose administered on embryonic day (E) 13.5. Whole-mount preparations of E18.5 embryos showed that joints in the vertebrae, forelimb, and hindlimb were marked (Figures S1Ab–S1Ad''), suggesting that Cre recombinase activity was indeed restricted to joints. Importantly, no reporter activity was evident without tamoxifen administration (Figures S1Ba–S1Bc).

Next, we crossed mice heterozygous for *Gdf5-CreER* and analyzed the homozygous offspring. As expected, the phenotype recapitulated that of *brachypodism (bp)* mice (Harada et al., 2007; Mikic, 2004; Storm et al., 1994); namely, malformation in the autopods and fibula, failure of cruciate ligament development, and expansion of the *Gdf5* expression domain in the autopod (Figures S1Ca–S1Ce'). Together, these results indicate that the *Gdf5-CreER* line is a suitable system for lineage analysis of *Gdf5*-positive interzone cells.

Joint-Forming Cells Are Not Specified in a Single Early Event

According to the interzone progenitor model, once the interzone has formed, the cells inside it are specified as joint progenitors, as indicated by *Gdf5* expression. This hypothesis predicts that administration of tamoxifen at that stage would "capture" most of the population of joint progenitors, resulting in cell labeling throughout the joint. To directly examine this hypothesis, we performed a series of pulse-chase experiments by crossing *Gdf5-CreER* mice with the *Rosa26-tdTomato* reporter. As seen in Figure 1A, on E11.5, *Gdf5* expression was clearly observed in the presumptive elbow, knee, and autopod joints. Assuming a 24-hr delay in maximum Cre activity, a single dose of tamoxifen was administered on E10.5 to label *Gdf5*-positive interzone cells. Interestingly, analysis of sections through the knee, elbow, and metacarpophalangeal joints on E18.5 showed only restricted labeling, mostly of epiphyseal cells (Figure 1B). This surprising result suggests that the *Gdf5*-positive cells that populate the interzone at the time of its formation are not the main source of joint progenitors.

An alternative hypothesis that could reconcile our observations with those obtained previously using the *Gdf5-Cre* line is that there is a constant inflow of new cells into the forming joint. The "influx" model predicts that a single administration of tamoxifen will mark only a partial population of joint cells and that only several administrations at different developmental stages will induce extensive labeling. To test this hypothesis, we administered three doses of tamoxifen on E11.5, E13.5, and E15.5. Examination of sections through several E18.5 joints showed that *tdTomato*-positive cells occupied most of the joint area (Figure 1C), thus reinforcing the influx hypothesis.

The interzone progenitor model implies a requirement for continuous proliferation of the progeny of early-specified *Gdf5*-positive progenitors throughout development to sustain rapid joint growth. To further distinguish between the two hypotheses, we examined the proliferative potential of these cells. We analyzed, by bromodeoxyuridine (BrdU) assay, the descendants of *Gdf5*-positive cells labeled by a single tamoxifen administration on E11.5. Sections through the elbow and knee joints showed that approximately 20% of the descendants, marked by tdTomato, were proliferating on E13.5. Moreover, the level of proliferation dramatically decreased through E15.5 and E18.5 (Figures 1D and 1E). Taken together, these results imply a continuous influx of cells into the forming joint.

Joint Development Involves a Continuous Influx of New *Gdf5*-Expressing Cells

Next, to directly demonstrate the recruitment process, we monitored the spatial distribution of *Gdf5* and *tdTomato* expression in the interzone during development. The probe for the *tdTomato* gene was expected to mark cells that have already been specified as *Gdf5*-positive at the time of tamoxifen administration and their descendants, whereas the probe for *Gdf5* would mark cells that expressed *Gdf5* at the time of harvesting. Thus, expression of both markers would indicate cells that were recruited early and maintained *Gdf5* expression, whereas newly recruited, non-pulsed cells would express only *Gdf5*. First, to verify the sensitivity of in situ hybridization (ISH) for *tdTomato*, we compared the results of that assay (red) with immunofluorescent staining for tdTomato protein (green) (Figure 2A). The co-localization of labeled cells showed that ISH for *tdTomato* is a reliable tool in cell lineage studies.

According to our model, immediately after Cre activation, interzone cells should express both *Gdf5* and *tdTomato.* To examine this assumption, we performed double ISH for both genes on sections from *Gdf5-CreER*, *Rosa26-tdTomato* embryos following administration of a single dose of tamoxifen at different time points during joint development (E11.5–E13.5). Embryos were harvested 28 hr after tamoxifen administration because we had expected a delayed activation of the Rosa26 reporter. In agreement with our hypothesis, sections through the knee showed a high overlap between *Gdf5*- and *tdTomato*-positive cells pulsed at all the time points (Figures 2B and S2).

To assess the efficiency of *Gdf5-CreER* recombination quantitatively, we measured the level of co-localization of *Gdf5*- and *tdTomato*-expressing cells. The results showed that 60%–67% of the *Gdf5* expression domain was also positive for *tdTomato* (Figure 2C). Surprisingly, 28 hr after tamoxifen administration, we already observed a population of *tdTomato*-positive, *Gdf5*-negative cells (Figure 2B, arrows). Assessment of the proportion of that population relative to the entire *tdTomato* expression domain showed that, at all examined stages, approximately 30% of *tdTomato*-positive cells had already lost *Gdf5* expression. This observation indicates a very dynamic cellular behavior and suggests that the actual recombination efficiency is higher than calculated (Figures 2C and 2D). Moreover, the coexpression of *Gdf5* and *tdTomato* by most cells after that interval

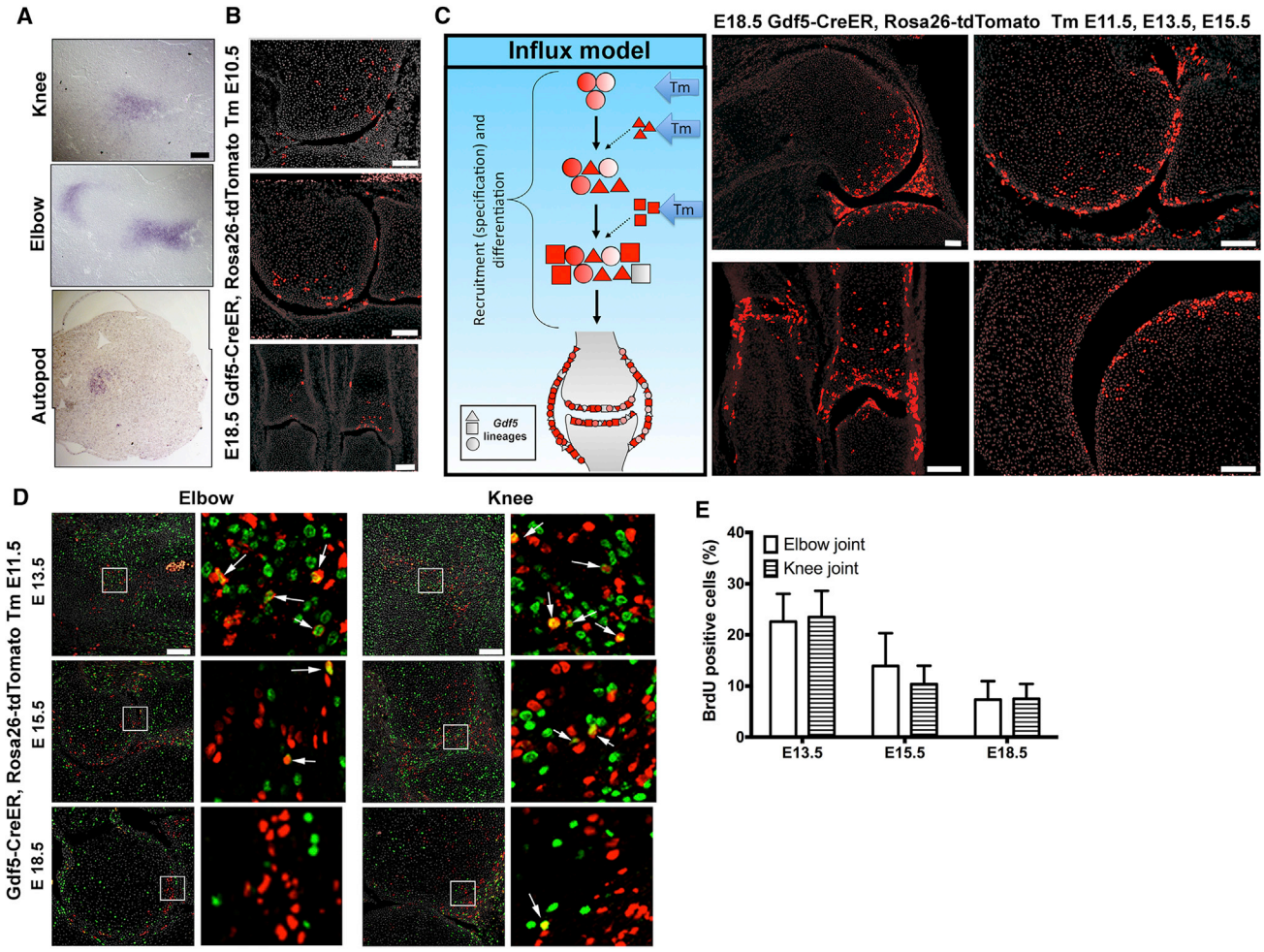

Figure 1. Limited Proliferation of *Gdf5*+ Lineage Cells Contradicts the Interzone Progenitor Hypothesis

(A) Sections through the knee, elbow, and autopod of E11.5 embryos show *Gdf5* expression in various joints.

(B) Pulse-chase lineage tracing experiment with a single dose of tamoxifen administered on E10.5 to mark approximately the same cell populations shown in (A). Sections through E18.5 *Gdf5-CreER*, *Rosa26-tdTomato* embryo knee, elbow, and metacarpophalangeal joints show that *tdTomato*-positive cells do not occupy most of the joint area.

(C) Left: illustration of the predicted outcome of multiple tamoxifen (Tm) administrations according to the influx model. Right: sections through E18.5 forelimb and hindlimb following repeated pulsing on E11.5, E13.5, and E15.5 show numerous *tdTomato*-positive cells at the knee (top left), elbow (top right), metacarpophalangeal (bottom left), and humeroscapular (bottom right) joints, consistent with the model.

(D) Pulse-chase experiment with a single dose of tamoxifen administered on E11.5. Shown is immunofluorescent staining for BrdU (green) and tdTomato (red) on sections through elbow and knee joints on E13.5, E15.5, and E18.5 (arrows indicate double-labeled cells).

(E) Quantification of the percentage of proliferating descendants of *Gdf5*-expressing cells on E13.5, E15.5, and E18.5.

Scale bars represent 100 μm.

demonstrated our ability to effectively detect the expression of both markers as well as the high level of Cre activity following a single tamoxifen administration.

Another prediction of our model is that longer pulse-chase intervals would reduce the overlap between the *Gdf5* and *tdTomato* expression domains as a result of *Gdf5* expression by cells recruited after pulsing. Indeed, examination of E13.5–E15.5 knee joints of embryos pulsed on E11.5 showed that, in addition to cells that co-expressed both markers, a high number of cells expressed only *Gdf5* but not *tdTomato* (Figure 2E, arrows). As in the previous experiment (Figure 2B), a third population of cells that solely expressed *tdTomato* was also identified, presumably having lost *Gdf5* expression. These results reveal a highly dynamic behavior of joint-forming cells; new cells turn *Gdf5* expression on, whereas others turn it off.

Because, in that experiment, tamoxifen was administered only on E11.5, the observed dynamic behavior could be unique to that developmental stage. To address that issue, we repeated the pulse-chase experiments, administering single doses of tamoxifen at different stages (E10.5–E13.5), and examined *tdTomato* and *Gdf5* expression in the knee joint on E15.5. In all experiments, the three abovementioned populations were detected (Figure 2F), indicating a continuous influx of *Gdf5*-positive cells into the joint.

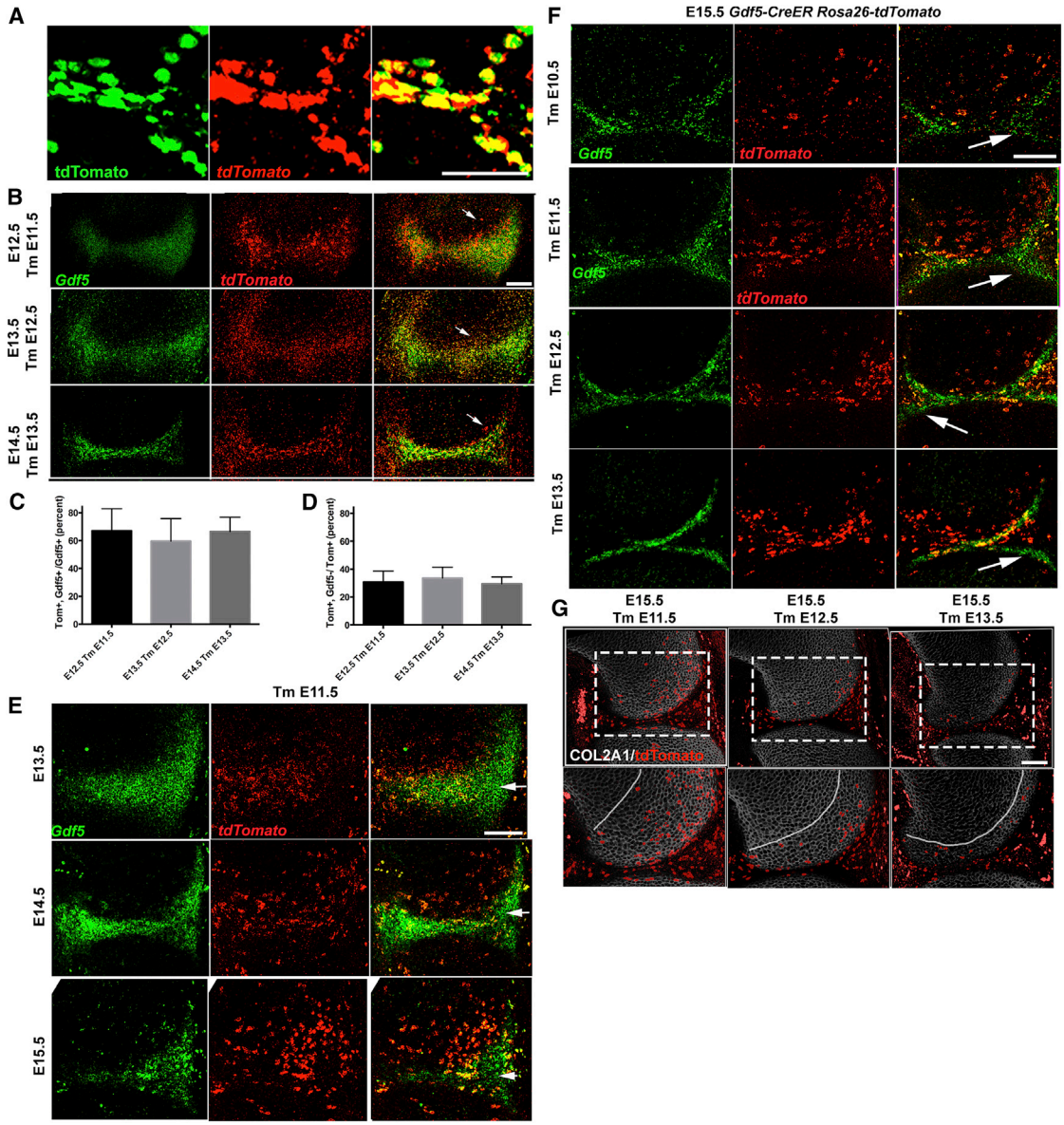

Figure 2. Joint Development Involves Continuous Steps of Recruitment and Specification of New Cells

(A) Immunofluorescent staining (green) and gene expression (red) of the tdTomato reporter demonstrate reliable detection of the reporter by ISH.

(B) Double ISH for *Gdf5* (green) and *tdTomato* (red) genes on E12.5–E14.5, following administration of a single tamoxifen dose on E11.5–E13.5, respectively, shows that almost the entire *Gdf5*-expressing population was genetically marked (arrows indicate *tdTomato*-positive, *Gdf5*-negative cells).

(C) Quantification of the percentage of *Gdf5*, *tdTomato* double-positive cells from all *Gdf5*-positive cells.

(D) Quantification of the percentage of *tdTomato*-positive, *Gdf5*-negative cells from all *tdTomato*-positive cells.

(E) Analysis of *Gdf5* (green) and *tdTomato* (red) expression on E13.5–E15.5, following tamoxifen administration on E11.5, shows dynamic expression patterns and the existence of newly recruited cells that express only *Gdf5* (arrows).

(F) Analysis of *Gdf5* and *tdTomato* gene expression in E15.5 knee joints following a single tamoxifen administration on E10.5–E13.5 shows that recruitment is a continuous process (newly recruited cells are indicated by arrows).

(G) Analysis of tdTomato (red) and COL2A1 (white) protein localization on an E15.5 knee joint following a single tamoxifen administration on E11.5–E13.5. Bottom: magnifications of the boxed areas at the top. Curved lines demarcate the epiphyseal domains where contribution of tdTomato-positive cells is seen.

Scale bars represent 50 μm (A) and 100 μm (B–G).

Finally, our finding that cells were constantly leaving the *Gdf5* expression domain suggested that the contribution of the *Gdf5* lineage to the developing epiphyses is more intricate and fine-tuned than has been appreciated previously (Koyama et al., 2007; Rountree et al., 2004; Storm and Kingsley, 1999). To better understand the temporal contribution of the *Gdf5* lineage to the epiphysis, we performed pulse-chase experiments using *Gdf5-CreER* mice crossed with *Rosa26-tdTomato* mice. Following

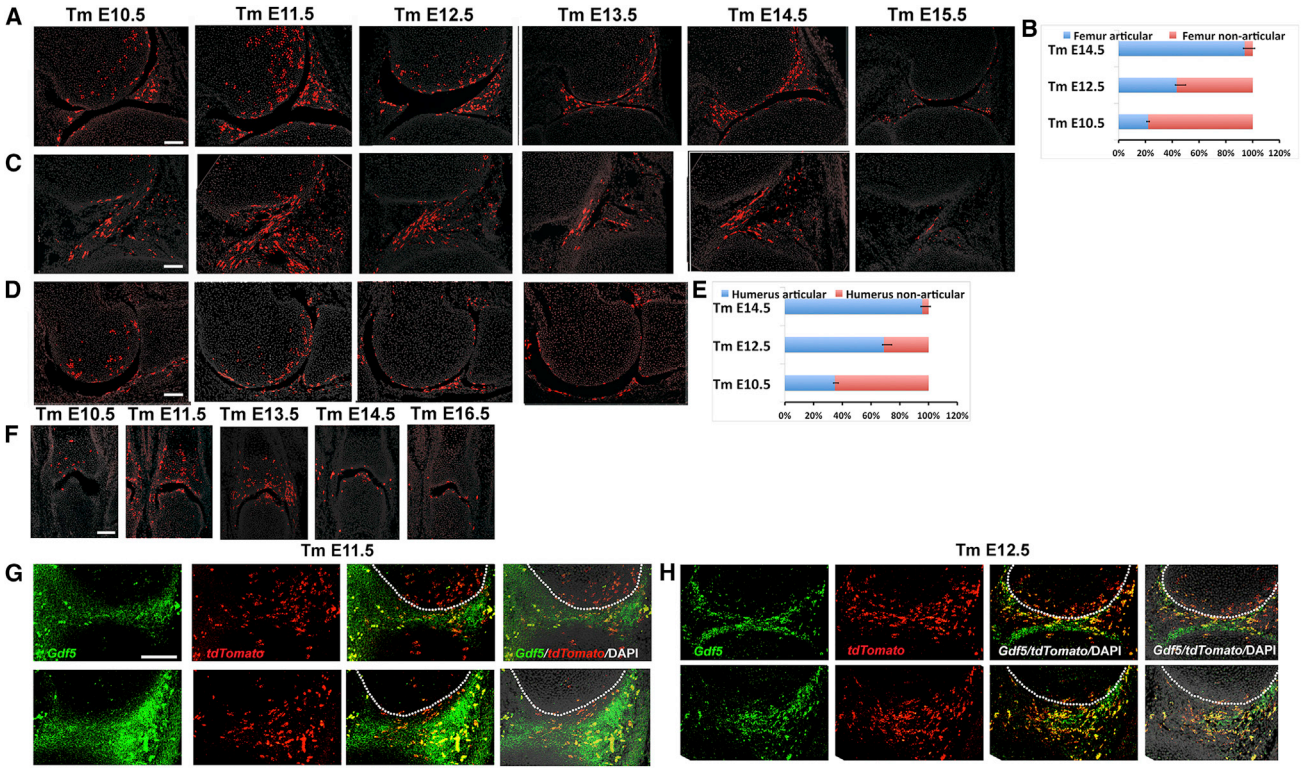

Figure 3. Differential Contribution of Cell Subpopulations to Various Joint Tissues

Pulse-chase experiments using *Gdf5-CreER*, *Rosa26-tdTomato* mice were performed.

(A, C, D, and F) Tamoxifen was administered at various stages between E10.5 and E16.5. Examination on E18.5 shows the contribution of different *Gdf5*-expressing pools to the developing knee (A and C), elbow (D), and metacarpophalangeal (F) joints.

(B and E) Quantification of the percentage of *tdTomato*-positive cells contributing to articular cartilage from all labeled cells at the distal femur (B) and distal humerus (E).

(G and H) Analysis of *Gdf5* (green) and *tdTomato* (red) expression in E15.5 medial knee sections through the meniscus (top) and mid-sagittal sections through the cruciate ligaments (bottom) following pulsing on E11.5 (G) and E12.5 (H) shows a substantial overlap in expression domains in the ligaments compared with the meniscus (dashed lines demarcate the femur epiphysis).

Scale bars represent 100 μm.

administration of a single dose of tamoxifen on E11.5–E13.5, E15.5 embryos were stained for both tdTomato and collagen type II α1 (COL2A1). Activation on E11.5 resulted in a substantial population of tdTomato, COL2A1 double-positive cells. Later marking of *Gdf5*-expressing populations by tamoxifen administration on E12.5–E13.5 (Figure 2G) resulted in a gradual decrease in labeling of epiphyseal chondrocytes and labeled chondrocytes more proximal to the joint, indicating a spatial shift toward the joint area. These results indicate that the cells lost their *Gdf5* expression (Figure 2F), joined the growing cartilage, and differentiated into chondrocytes (Figure 2G).

This set of experiments shows that the *Gdf5* expression domain is highly dynamic, with a constant influx of new cells into the joint area as well as out of it into the epiphyses.

The Influx of Cells into the Joint Facilitates Lineage Divergence

A possible implication of the influx model is that *Gdf5*-positive cells recruited at different time points may give rise to specific joint tissues. To address this hypothesis, we analyzed the spatiotemporal contribution of cell lineages marked at different stages to various joints of E18.5 embryos. For that, we administered single doses of tamoxifen between E10.5 and E16.5 to embryos heterozygous for *Gdf5-CreER* and *Rosa26-tdTomato*. As seen in Figure 3, descendants of *Gdf5*-positive cells marked at different time points populated different regions of the developing joints.

In the knee, *Gdf5*-positive cells were detected in the epiphyses, articular cartilage, meniscus, and intra-articular ligaments. Early tamoxifen administration (on E10.5) resulted in *tdTomato*-positive cells located mostly at the epiphyses. However, when tamoxifen was administered at E11.5, *tdTomato*-positive cells were also observed in the articular cartilage. Upon activation on E12.5–E13.5, the number of *tdTomato*-positive cells in the epiphyses decreased, whereas their relative number in the articular cartilage increased. Finally, following activation on E14.5–E15.5, the expression was restricted to the most superficial layer of the articular cartilage (Figures 3A and 3B). Tamoxifen administration at all stages led to a contribution of *tdTomato*-positive cells to the meniscus and intra-articular ligaments. However, whereas pulsing at early and intermediate stages led to a massive contribution throughout

the tissues, at later stages it resulted in an exclusive contribution of these cells to the edges of the meniscus (Figure 3A) and intra-articular ligament (Figure 3C).

In the elbow joint, a similar trend was observed, except that a contribution of *Gdf5*-positive cells to the articular cartilage was observed following activation on E12.5 (Figures 3D and 3E). The metacarpophalangeal joint also exhibited a similar spatiotemporal pattern. However, administration on E13.5 (Figure 3F) resulted in prominent labeling of the joint capsule. Finally, the different contribution of labeled cells to epiphyseal chondrocytes seen in knee sections (Figures 3A and 3C) prompted us to further examine the spatial distribution of *Gdf5*- and *tdTomato*-expressing cells in E15.5 embryos pulsed on E11.5 (Figure 3G) or E12.5 (Figure 3H). Mid-sagittal sections through the knee, where the cruciate ligaments were visualized, revealed significantly more cells that expressed both genes (Figures 3G and 3H, bottom) and a clear reduction in *tdTomato*-positive, *Gdf5*-negative cells compared with medial sections showing the menisci. Presumably, the latter cell population highly contributes to the epiphysis (Figures 3G and 3H, top).

Importantly, in all joints we observed asymmetry in the contribution of *Gdf5*-positive cells to the skeletal elements at the two sides of the joint. For example, the femur and the humerus were more extensively marked than the opposing bones. This observation suggests that asymmetric contribution may be part of the morphogenetic process (Figure 1C).

Overall, the spatiotemporal differences in *Gdf5* expression patterns show the dynamics of the establishment of the different joint tissues. Although some elements, like the cruciate ligaments and menisci, are formed by constant recruitment of new *Gdf5*-expressing cells that maintain its expression, others, like the metacarpophalangeal joint capsule, originate from a temporally specific group of cells. It is tempting to speculate that this mode of development may facilitate lineage divergence into different cell fates to allow the formation of the various tissues that compose the joint.

A Continuous Influx of *Sox9*-Positive Cells May Contribute to Joint Morphogenesis

Previously, it was shown that joint cells originate from *Sox9*-positive chondroprogenitor cells (Soeda et al., 2010). To confirm this, we crossed *Sox9-CreER* mice with the *Rosa26-tdTomato* reporter. Examination of E15.5 knee and elbow joints following administration of a single tamoxifen dose at E10.5 showed that all structures of the joints were *tdTomato*-positive, thus originating from an early population of *Sox9*-positive cells (Figures S3Aa–S3Ad). To further establish that *Gdf5*-positive cells are derived from that early pool, double ISH for *tdTomato* and *Gdf5* was performed on sections through the knee of *Sox9-CreER*, *Rosa26-tdTomato* heterozygous embryos. The co-expression of both markers confirmed that conclusion (Figure S3Ae).

Several studies have suggested that cells from the vicinity may migrate into the developing joint (Hyde et al., 2008; Koyama et al., 2007; Pacifici et al., 2006; Ray et al., 2015). To locate the source that may supply new cells to the developing joint, we next analyzed the expression of the two abovementioned genes alongside COL2A1, a marker of differentiating chondrocytes, throughout joint development. To visualize all three markers simultaneously, double ISH for *Sox9* and *Gdf5* was performed together with immunofluorescence staining for COL2A1. Examination of the elbow and knee joints at E12 revealed, as expected, a population of *Sox9-Gdf5* double-positive cells at the presumptive joint area. This population was later observed at all examined stages (Figures 4A–4F and S3Ca–S3Cf). However, around the developing joint, we observed a cloud of *Sox9*-positive cells that did not express *Col2a1* or *Gdf5* (Figures 4A and S3Ca). That population was also prominent in double immunofluorescence staining for SOX9 and COL2A1 (Figure S3B).

As development proceeded, two concurrent events were observed: massive growth and morphogenesis of the joint and a gradual reduction in the population of *Sox9*-positive, *Col2a1*, *Gdf5*-negative cells around the joint (Figures 4A–4F and S3Ca–S3Cf; arrows), which was also confirmed by immunofluorescent staining (Figure S3B). Interestingly, in the interzone, between the *Col2a1*-positive cells that flanked it and the *Gdf5* expression domain, another population of cells that was *Sox9*-positive and *Col2a1, Gdf5*-negative was observed (Figures 4C, 4D, and S3C; dashed arrows). These cells were likely descendants of early *Gdf5*-positive cells that had lost *Gdf5* expression, as we demonstrated previously (Figure 2), and were in the process of differentiation to chondrocytes while integrating into the epiphyses (Figure S3D).

Together, these results suggest that *Sox9*-positive, *Col2a1*, *Gdf5*-negative cells from the vicinity of the joint migrate into the forming joint, turn on *Gdf5* expression, and contribute to joint development.

DISCUSSION

Over the years, a general scheme of organogenesis has been widely adopted. This scheme has guided efforts to trace the lineages of organ-forming cells to identify their progenitors. In accordance with this view, *Gdf5*-positive interzone cells have been suggested as joint progenitors. However, the data we present here are inconsistent with the progenitor model sensu stricto and favor an alternative strategy for joint development that involves a constant influx of new cells that are integrated into the forming organ to sustain its development.

Several lines of evidence in our study are inconsistent with the view that joint progenitor cells are all specified at an early stage of limb development. None of our attempts, using a knockin *Gdf5-CreER* line, to capture the entire progenitor population by a single Cre activation succeeded; each time, only a certain subpopulation of joint cells was marked. Only several doses of tamoxifen at different developmental stages resulted in extensive labeling throughout the joint. Moreover, cell proliferation assays revealed a reduction in the proliferation of the *Gdf5* lineage through development that could not accommodate the demands of the developing joint. Finally, our finding of a time-dependent increase in the number of new *Gdf5*-positive cells in the interzone may also be incompatible with the progenitor model.

A possible limitation of our approach would be low recombination activity of the new *Gdf5-CreER* line, which would lead to low

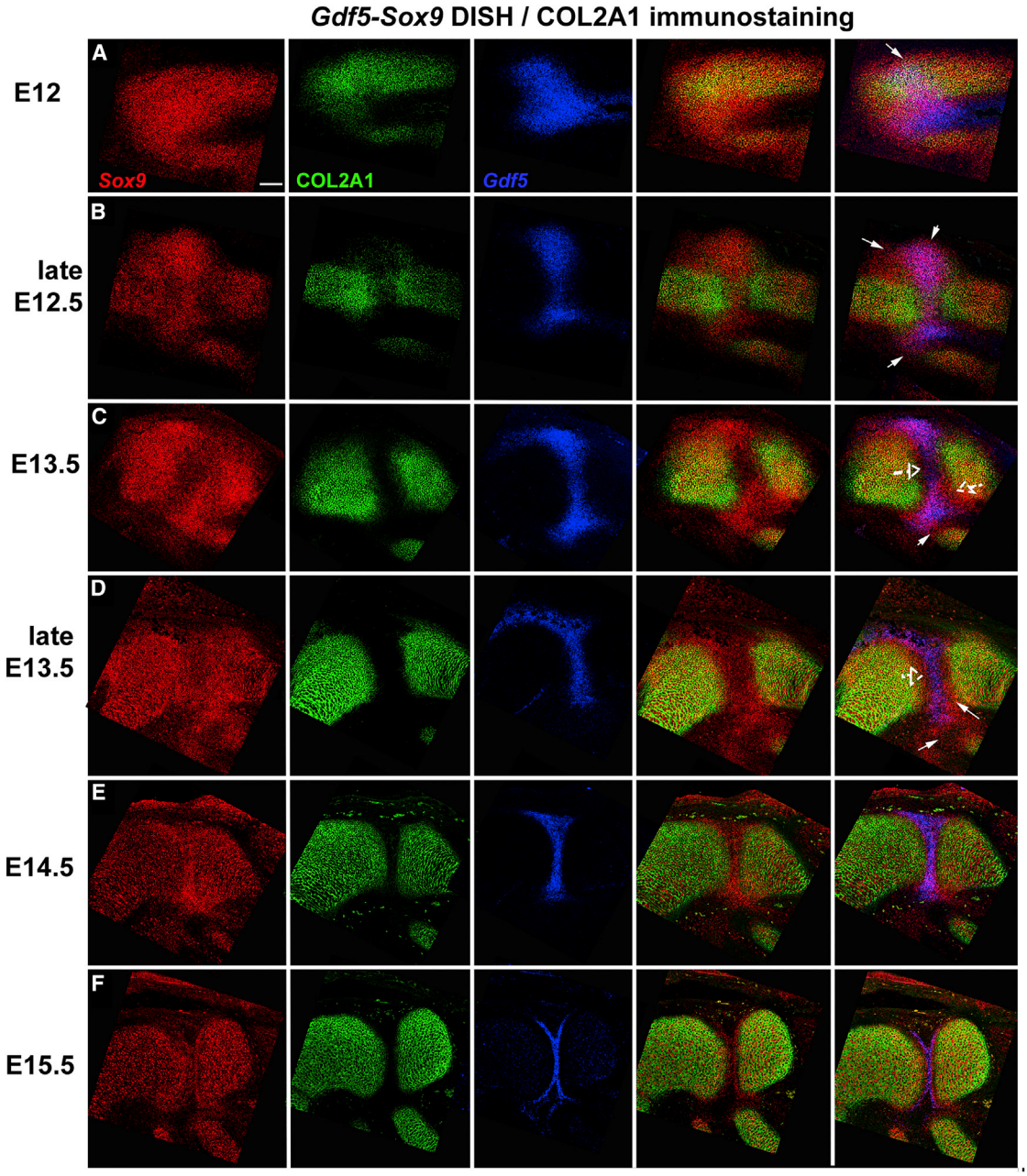

Figure 4. Gene Expression Dynamics Suggests that Influx of Sox9-Positive Cells Contributes to Joint Formation

(A–F) *Gdf5* and *Sox9* double ISH and COL2A1 immunofluorescent staining on sections through E12–E15.5 knee joints. Arrows indicate a population of *Sox9*-positive *Gdf5*, COL2A1-negative cells outside (solid arrows) and inside (dashed arrows) of the interzone. Scale bars represent 100 μm.

labeling efficacy. However, comparable levels of *tdTomato* and endogenous *Gdf5* expression observed and computed shortly after Cre activation suggest that our new line acts efficiently on the *Rosa26-tdTomato* reporter line.

The concept of the addition of cells to a developing organ instead of relying exclusively on proliferation of progenitor cells is interesting. Previously, we showed that cells that form bone eminences and the patella are added secondarily to the already established bone shaft anlage (Blitz et al., 2009, 2013; Eyal et al., 2015). Although these studies fall short of providing direct evidence for the continuity of this process, the different timing suggests that the influx model may be a broader phenomenon in skeletal development.

Intriguingly, our findings may appear to disagree with Holder's seminal experiment in which removal of the interzone led to failure in joint development (Holder, 1977). There are several

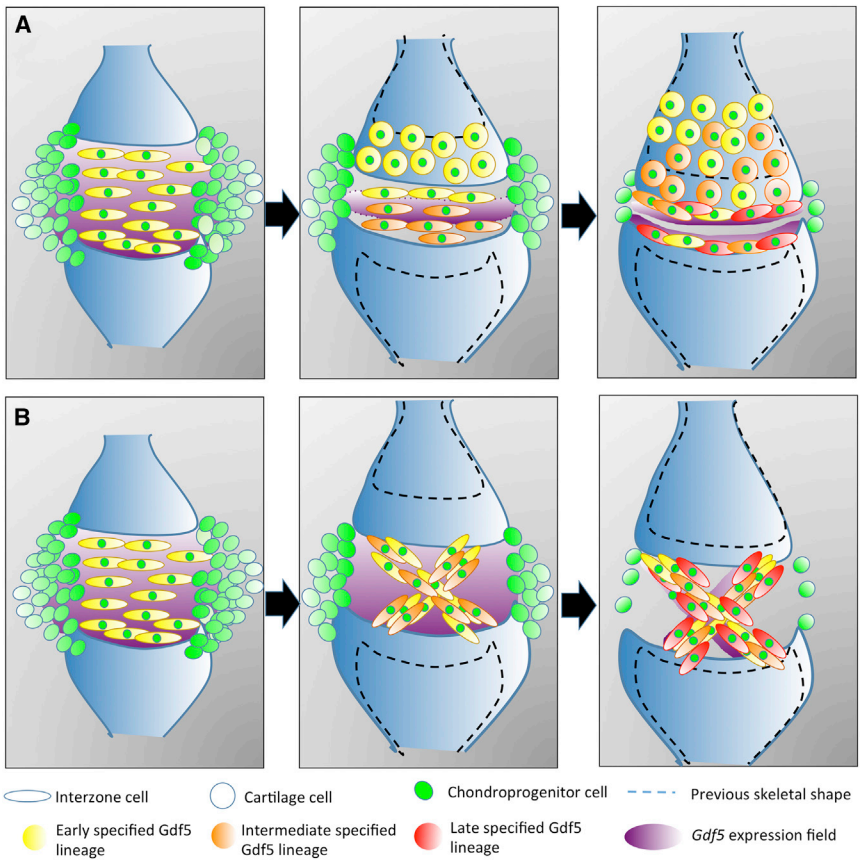

Figure 5. A Revised Model for Joint Development

Joint development involves constant specification of new *Gdf5*-positive cells from *Sox9*-expressing chondroprogenitors.

(A) These cells exhibit a highly dynamic behavior. Thus, some early-specified cells (yellow) will quickly lose *Gdf5* expression and contribute to the growing epiphyses more than later-recruited cells (orange and red).

(B) In contrast, the constant influx of specified cells that are destined to contribute to the intra-articular ligaments will maintain *Gdf5* expression and their localization to the developing joint site.

possible ways for reconciling these seemingly opposing conclusions. For example, Holder might have removed with the interzone the surrounding tissues, including the potential source for migrating *Gdf5*-positive cells, leading to failure in joint development. Also, several lines of evidence support the notion that the interzone is a vital signaling center in joint development (Decker et al., 2014; Longobardi et al., 2015). Thus, removal of the interzone could have eliminated the regulatory signals mediating the recruitment process. A third possibility is that Holder also removed muscles, which were shown previously by us and others to be essential for joint development (Kahn et al., 2009; Nowlan et al., 2010; Pitsillides and Ashhurst, 2008; Shwartz et al., 2013).

A central question in organ development is the mechanism by which lineage divergence occurs to form different tissues. This question is particularly interesting in the case of joint development because all joint tissues were shown to originate from *Gdf5*-expressing cells (Koyama et al., 2007, 2008; Rountree et al., 2004). Previous studies have suggested two possible mechanisms for the divergence into epiphyseal and articular chondrocytes based on either temporal or spatial differences. The temporal hypothesis is that cells that express *Gdf5* early will contribute to the epiphysis (Storm and Kingsley, 1999), whereas the spatial hypothesis is that the location of the progenitors in the interzone determines the ultimate lineage destination (Ito and Kida, 2000). We propose the high cellular dynamics of *Gdf5* expression as the underlying factor of tissue divergence.

Although the mechanism that translates *Gdf5* expression dynamics to lineage divergence is yet to be deciphered, we identify two important parameters, the duration and time of onset of *Gdf5* expression, whose combination may determine lineage divergence (Figure 5). For example, cells that would eventually contribute to the epiphysis lost *Gdf5* expression, whereas cells that contributed to the meniscus and knee cruciate ligaments exhibited completely different dynamics and maintained *Gdf5* expression. Interestingly, articular cartilage was also found to express *Gdf5* continually. However, the recruitment of most of these cells started 1 day later than in the ligaments and menisci. This differential behavior can serve as a mechanism by which cells contributing to different joint tissues acquire their fate (Figure 5). This notion is supported by previous studies showing that *Gdf5* is essential for the development of intra-articular ligaments (Harada et al., 2007), which were absent in *bp* mice, and that human mesenchymal stem cells (hMSCs) and murine adipose tissue-derived mesenchymal stem cells treated with GDF5 showed an elevation in tendon-specific markers such as scleraxis (*Scx*) (Park et al., 2010; Tan et al., 2012). An example for the onset of *Gdf5* expression as a cue for lineage divergence is the case of the metacarpophalangeal joint capsule, where the contributing cells start to express this gene only on E13.5.

The influx of new cells and the dynamic behavior of joint-forming, *Gdf5*-expressing cells may provide flexibility both in development and during evolution. Various joint structures support specific functions and mechanical needs. Development through multiple steps, some of which are lineage-specific, may enable faster and more efficient changes in joint structure by manipulating only a subpopulation of joint-forming cells.

A key question that remains to be solved is the source of the recruited cells. Previous studies have shown that all joint structures originate from matrilin 1-negative (Hyde et al., 2007) and *Sox9*-positive cells (Soeda et al., 2010). Other works indicate that cells

are recruited into the developing joint (Hyde et al., 2008; Koyama et al., 2007; Pacifici et al., 2006; Ray et al., 2015). Our study identifies a population of *Sox9*-positive, *Col2a1*, *Gdf5*-negative cells outside of the joint area that may serve as an external source. However, this supposition is yet to be conclusively confirmed. Another possibility is an internal origin correlating to the *Sox9*-positive, *Col2a1*, *Gdf5*-negative cells we observed in the interzone. However, we believe that there are several indications for recruitment from an outside source.

First, the *Gdf5* expression domain is initially very broad, occupying the entire interzone and leaving no room for *Sox9*+, *Gdf5*−, *Col2a1*− cells to contribute to the *Gdf5*-expressing population. Moreover, as we demonstrate, the CreER^{T2} system is highly efficient and is thus likely to mark the majority of *Gdf5*-positive interzone cells. Nonetheless, we cannot rule out the possibility that a unique subpopulation of unlabeled *Gdf5*-positive interzone cells contributes to joint growth and, as an internal source, to cell recruitment. Last, we demonstrate a clear decrease in the number of *Sox9*+, *Gdf5*− cells flanking the forming joint during development, supporting the argument that this population is the source for joint cells.

Interestingly, a recent study by Ray et al. (2015) suggests that articular cartilage originates from proliferating chondrocytes, proposing another possible source outside of the interzone. However, because a different system was used in that study, the *Col2a1-CreER*^{T2} mouse, the exact spatial and temporal relationships between the process identified by Ray et al. (2015) and the one described here are yet to be determined. A plausible explanation for the apparent differences is that both these processes contribute to joint formation in varying proportions. Thus, examination of different joints at different time points may yield inconsistent results.

From a medical perspective, joints exhibit a very limited capacity for regeneration (Iwamoto et al., 2013; Sandell, 2012). Our results suggest that, to improve regeneration, it may be necessary to search for a mechanism that can enhance or activate cell recruitment.

In conclusion, our findings indicate that joints do not form from a single pool of early-specified *Gdf5*-positive cells but, rather, through a continuous influx of *Gdf5*-positive cells, hence the term influx model. Moreover, we show highly dynamic spatiotemporal patterns of *Gdf5* expression by interzone cells, which may serve as differentiation cues. An additional differentiation signal may be the temporal specification of cells that will contribute differentially to the various tissues of the mature joint, thus facilitating lineage divergence of *Gdf5*-positive cells.

EXPERIMENTAL PROCEDURES

Animals

All experiments involving mice were approved by the Institutional Animal Care and Use Committee (IACUC) of the Weizmann Institute. *Rosa26-tdTomato* mice (B6;129S6-*Gt(ROSA)26Sortm9(CAG-tdTomato)Hze*/J) have been described previously (Madisen et al., 2010; Soeda et al., 2010). The generation of *Gdf5-CreER* knockin mice is described in the Supplemental Experimental Procedures. To create *Gdf5-CreER, Rosa26-tdTomato* mice, floxed *Rosa26-tdTomato* mice were mated with *Gdf5-CreER* mice.

For harvesting of embryos, timed pregnant females were sacrificed by cervical dislocation.

Tamoxifen Administration

Pregnant female mice were administered 0.12–0.18 mg/g tamoxifen/body weight in corn oil by oral gavage.

Cryosectioning

Embryos were fixed in 4% paraformaldehyde (PFA)/PBS for 3 hr at 4°C, washed overnight in 30% sucrose/PBS at 4°C, embedded in O.C.T., and sectioned at a thickness of 10 μm.

Immunofluorescent Staining

For paraffin section immunofluorescence, embryos were fixed overnight in 4% PFA/PBS, dehydrated to 100% ethanol, embedded in paraffin, and sectioned at a thickness of 7 μm. 10 mM sodium citrate (pH 6.0) was used for antigen retrieval. Slides were incubated overnight at 4°C with primary antibody anti-BrdU (AbD) diluted 1:200 and with biotinylated anti-RFP (Abcam) diluted 1:100 in blocking solution to visualize tdTomato. For COL2A1 and tdTomato double immunostaining, after staining for tdTomato, slides were subjected to additional digestion by Proteinase K (Sigma). Slides were incubated overnight at 4°C with the primary antibody anti-COL2 (Developmental Studies Hybridoma Bank [DSHB], University of Iowa) 1:50 in blocking solution.

Following fluorescence ISH, slides were incubated overnight at 4°C with the primary antibody anti-COL2 (DSHB) 1:50 in blocking solution or with anti-RFP (Abcam) diluted 1:100 in blocking solution to visualize tdTomato.

In Situ Hybridization

Non-fluorescent ISH on paraffin sections was performed using a digoxigenin (DIG)-labeled probe for *Gdf5*. Double fluorescence ISH on paraffin sections was performed using fluorescein- and DIG-labeled probes. The extended protocol was described by Shwartz and Zelzer (2014).

BrdU Administration

Mice were injected intraperitoneally with 100 mg/kg of body weight BrdU labeling reagent (Sigma) and sacrificed 4 hr later. Forelimbs and hindlimbs were fixed in 4% PFA overnight at 4°C, dehydrated in ethanol, and embedded in paraffin.

Cell Count

For calculation of the percentage of tdTomato-positive cells contributing to the articular cartilage, 10-μm thick cryosections were counterstained with DAPI. tdTomato-positive cells were manually counted at the distal femoral and humeral heads as well as at the articular cartilage area, identified histologically as the external four to five cell layers. The percentage was calculated for each photographed section and averaged first for each embryo and then for each analyzed stage of tamoxifen administration.

To test the proliferation of tdTomato-positive cells, tdTomato-positive and tdTomato-BrdU-double positive cells were counted manually in BrdU-, RFP-, and DAPI-stained paraffin sections. In both experiments, 3-12 sections of each joint from each embryo were used, and three embryos from different litters were analyzed for each embryonic stage. Sections were photographed and examined by an LSM 710 or 780 confocal microscope. Data are represented as mean ± SD.

Co-localization Measurements

Section double ISH for *tdTomato* and *Gdf5* was imaged with an LSM 710 or 780 confocal microscope. The co-localization analysis was performed using the Imaris 8.2 colocalization module. For each analyzed picture, a region of interest covering the entire area of the knee joint containing *tdTomato*- and *Gdf5*-positive cells was defined and used for all measurements. Two to eleven sections of each joint from each embryo were used, and two to three embryos from two to three different litters were analyzed for each embryonic stage. The results represent all measured values ± SD.

SUPPLEMENTAL INFORMATION

Supplemental Information includes Supplemental Experimental Procedures and three figures and can be found with this article online at http://dx.doi.org/10.1016/j.celrep.2016.05.055.

AUTHOR CONTRIBUTIONS

Y.S., S.V., and S.K. conducted the experiments. E.Z. and Y.S. designed the study and wrote the manuscript.

ACKNOWLEDGMENTS

We thank N. Konstantin for expert editorial assistance. We thank Dr. Reinat Nevo for help with the co-localization analysis and all members of the E.Z. laboratory for advice and suggestions. This study was funded by the European Research Council (ERC; grant no. 310098), the Jeanne and Joseph Nissim Foundation for Life Sciences Research, the Y. Leon Benoziyo Institute for Molecular Medicine, Beth Rom-Rymer, the Estate of David Levinson, the Jaffe Bernard and Audrey Foundation, Georges Lustgarten, and the David and Fela Shapell Family Foundation.

Received: December 22, 2015
Revised: April 28, 2016
Accepted: May 15, 2016
Published: June 9, 2016

REFERENCES

Biehs, B., Hu, J.K., Strauli, N.B., Sangiorgi, E., Jung, H., Heber, R.P., Ho, S., Goodwin, A.F., Dasen, J.S., Capecchi, M.R., and Klein, O.D. (2013). BMI1 represses Ink4a/Arf and Hox genes to regulate stem cells in the rodent incisor. Nat. Cell Biol. *15*, 846–852.

Blitz, E., Viukov, S., Sharir, A., Shwartz, Y., Galloway, J.L., Pryce, B.A., Johnson, R.L., Tabin, C.J., Schweitzer, R., and Zelzer, E. (2009). Bone ridge patterning during musculoskeletal assembly is mediated through SCX regulation of Bmp4 at the tendon-skeleton junction. Dev. Cell *17*, 861–873.

Blitz, E., Sharir, A., Akiyama, H., and Zelzer, E. (2013). Tendon-bone attachment unit is formed modularly by a distinct pool of Scx- and Sox9-positive progenitors. Development *140*, 2680–2690.

Decker, R.S., Koyama, E., and Pacifici, M. (2014). Genesis and morphogenesis of limb synovial joints and articular cartilage. Matrix Biol. *39*, 5–10.

Eyal, S., Blitz, E., Shwartz, Y., Akiyama, H., Schweitzer, R., and Zelzer, E. (2015). On the development of the patella. Development *142*, 1831–1839.

Garrison, A.P., Helmrath, M.A., and Dekaney, C.M. (2009). Intestinal stem cells. J. Pediatr. Gastroenterol. Nutr. *49*, 2–7.

Gu, G., Dubauskaite, J., and Melton, D.A. (2002). Direct evidence for the pancreatic lineage: NGN3+ cells are islet progenitors and are distinct from duct progenitors. Development *129*, 2447–2457.

Guo, X., Day, T.F., Jiang, X., Garrett-Beal, L., Topol, L., and Yang, Y. (2004). Wnt/beta-catenin signaling is sufficient and necessary for synovial joint formation. Genes Dev. *18*, 2404–2417.

Harada, M., Takahara, M., Zhe, P., Otsuji, M., Iuchi, Y., Takagi, M., and Ogino, T. (2007). Developmental failure of the intra-articular ligaments in mice with absence of growth differentiation factor 5. Osteoarthritis Cartilage *15*, 468–474.

Hartmann, C., and Tabin, C.J. (2001). Wnt-14 plays a pivotal role in inducing synovial joint formation in the developing appendicular skeleton. Cell *104*, 341–351.

Holder, N. (1977). An experimental investigation into the early development of the chick elbow joint. J. Embryol. Exp. Morphol. *39*, 115–127.

Hyde, G., Dover, S., Aszodi, A., Wallis, G.A., and Boot-Handford, R.P. (2007). Lineage tracing using matrilin-1 gene expression reveals that articular chondrocytes exist as the joint interzone forms. Dev. Biol. *304*, 825–833.

Hyde, G., Boot-Handford, R.P., and Wallis, G.A. (2008). Col2a1 lineage tracing reveals that the meniscus of the knee joint has a complex cellular origin. J. Anat. *213*, 531–538.

Ito, M.M., and Kida, M.Y. (2000). Morphological and biochemical re-evaluation of the process of cavitation in the rat knee joint: cellular and cell strata alterations in the interzone. J. Anat. *197*, 659–679.

Iwamoto, T., Matsumura, N., Sato, K., Momohara, S., Toyama, Y., and Nakamura, T. (2013). An obliquely placed headless compression screw for distal interphalangeal joint arthrodesis. J. Hand Surg. Am. *38*, 2360–2364.

Kahn, J., Shwartz, Y., Blitz, E., Krief, S., Sharir, A., Breitel, D.A., Rattenbach, R., Relaix, F., Maire, P., Rountree, R.B., et al. (2009). Muscle contraction is necessary to maintain joint progenitor cell fate. Dev. Cell *16*, 734–743.

Koyama, E., Ochiai, T., Rountree, R.B., Kingsley, D.M., Enomoto-Iwamoto, M., Iwamoto, M., and Pacifici, M. (2007). Synovial joint formation during mouse limb skeletogenesis: roles of Indian hedgehog signaling. Ann. N Y Acad. Sci. *1116*, 100–112.

Koyama, E., Shibukawa, Y., Nagayama, M., Sugito, H., Young, B., Yuasa, T., Okabe, T., Ochiai, T., Kamiya, N., Rountree, R.B., et al. (2008). A distinct cohort of progenitor cells participates in synovial joint and articular cartilage formation during mouse limb skeletogenesis. Dev. Biol. *316*, 62–73.

Little, M.H. (2011). Renal organogenesis: what can it tell us about renal repair and regeneration? Organogenesis *7*, 229–241.

Longobardi, L., Li, T., Tagliafierro, L., Temple, J.D., Willcockson, H.H., Ye, P., Esposito, A., Xu, F., and Spagnoli, A. (2015). Synovial joints: from development to homeostasis. Curr. Osteoporos. Rep. *13*, 41–51.

Madisen, L., Zwingman, T.A., Sunkin, S.M., Oh, S.W., Zariwala, H.A., Gu, H., Ng, L.L., Palmiter, R.D., Hawrylycz, M.J., Jones, A.R., et al. (2010). A robust and high-throughput Cre reporting and characterization system for the whole mouse brain. Nat. Neurosci. *13*, 133–140.

Mikic, B. (2004). Multiple effects of GDF-5 deficiency on skeletal tissues: implications for therapeutic bioengineering. Ann. Biomed. Eng. *32*, 466–476.

Mitrovic, D.R. (1977). Development of the metatarsophalangeal joint of the chick embryo: morphological, ultrastructural and histochemical studies. Am. J. Anat. *150*, 333–347.

Nowlan, N.C., Sharpe, J., Roddy, K.A., Prendergast, P.J., and Murphy, P. (2010). Mechanobiology of embryonic skeletal development: Insights from animal models. Birth Defects Res. C Embryo Today *90*, 203–213.

Pacifici, M., Koyama, E., Shibukawa, Y., Wu, C., Tamamura, Y., Enomoto-Iwamoto, M., and Iwamoto, M. (2006). Cellular and molecular mechanisms of synovial joint and articular cartilage formation. Ann. N Y Acad. Sci. *1068*, 74–86.

Park, A., Hogan, M.V., Kesturu, G.S., James, R., Balian, G., and Chhabra, A.B. (2010). Adipose-derived mesenchymal stem cells treated with growth differentiation factor-5 express tendon-specific markers. Tissue Eng. Part A *16*, 2941–2951.

Pitsillides, A.A., and Ashhurst, D.E. (2008). A critical evaluation of specific aspects of joint development. Dev. Dyn. *237*, 2284–2294.

Ray, A., Singh, P.N., Sohaskey, M.L., Harland, R.M., and Bandyopadhyay, A. (2015). Precise spatial restriction of BMP signaling is essential for articular cartilage differentiation. Development *142*, 1169–1179.

Rountree, R.B., Schoor, M., Chen, H., Marks, M.E., Harley, V., Mishina, Y., and Kingsley, D.M. (2004). BMP receptor signaling is required for postnatal maintenance of articular cartilage. PLoS Biol. *2*, e355.

Sandell, L.J. (2012). Etiology of osteoarthritis: genetics and synovial joint development. Nat. Rev. Rheumatol. *8*, 77–89.

Shwartz, Y., and Zelzer, E. (2014). Nonradioactive in situ hybridization on skeletal tissue sections. Methods Mol. Biol. *1130*, 203–215.

Shwartz, Y., Blitz, E., and Zelzer, E. (2013). One load to rule them all: mechanical control of the musculoskeletal system in development and aging. Differentiation *86*, 104–111.

Soeda, T., Deng, J.M., de Crombrugghe, B., Behringer, R.R., Nakamura, T., and Akiyama, H. (2010). Sox9-expressing precursors are the cellular origin of the cruciate ligament of the knee joint and the limb tendons. Genesis *48*, 635–644.

Später, D., Hill, T.P., Gruber, M., and Hartmann, C. (2006). Role of canonical Wnt-signalling in joint formation. Eur. Cell. Mater. *12*, 71–80.

Stanger, B.Z., Tanaka, A.J., and Melton, D.A. (2007). Organ size is limited by the number of embryonic progenitor cells in the pancreas but not the liver. Nature *445*, 886–891.

Storm, E.E., and Kingsley, D.M. (1999). GDF5 coordinates bone and joint formation during digit development. Dev. Biol. *209*, 11–27.

Storm, E.E., Huynh, T.V., Copeland, N.G., Jenkins, N.A., Kingsley, D.M., and Lee, S.J. (1994). Limb alterations in brachypodism mice due to mutations in a new member of the TGF beta-superfamily. Nature *368*, 639–643.

Tan, S.L., Ahmad, R.E., Ahmad, T.S., Merican, A.M., Abbas, A.A., Ng, W.M., and Kamarul, T. (2012). Effect of growth differentiation factor 5 on the proliferation and tenogenic differentiation potential of human mesenchymal stem cells in vitro. Cells Tissues Organs (Print) *196*, 325–338.

Wilkinson, A.C., and Göttgens, B. (2013). Transcriptional regulation of haematopoietic stem cells. In Transcriptional and Translational Regulation of Stem Cells: Advances in Experimental Medicine and Biology, G. Hime and H. Abud, eds. (Springer), pp. 187–212.

Cell Reports, Volume *15*

Supplemental Information

Joint Development Involves a Continuous Influx of Gdf5-Positive Cells

Yulia Shwartz, Sergey Viukov, Sharon Krief, and Elazar Zelzer

Inventory of Supplemental Information

Supplemental Figures

Figure S1 shows the generation and validation of the *Gdf5-CreER* model system **(Figure 1)** by demonstrating the requirement of tamoxifen to induce reporter activity and by showing that homozygous embryos exhibit a phenotype recapitulating that of *Gdf5*-null mice.

Figure S2 provides magnifications of the double ISH for *Gdf5* and *tdTomato* shown in **Figure 2.**

Figure S3 supports the argument that an influx of *Sox9*-positive cells contributes to joint formation **(Figure 4)** by pulse-chase experiments on *Sox9-CreER* mice crossed with *Rosa26-tdTomato* reporter mice ,by double immunofluorescent staining for COL2A1 and SOX9 and by showing a similar gene expression dynamic in the elbow joint as was shown for the knee joint.

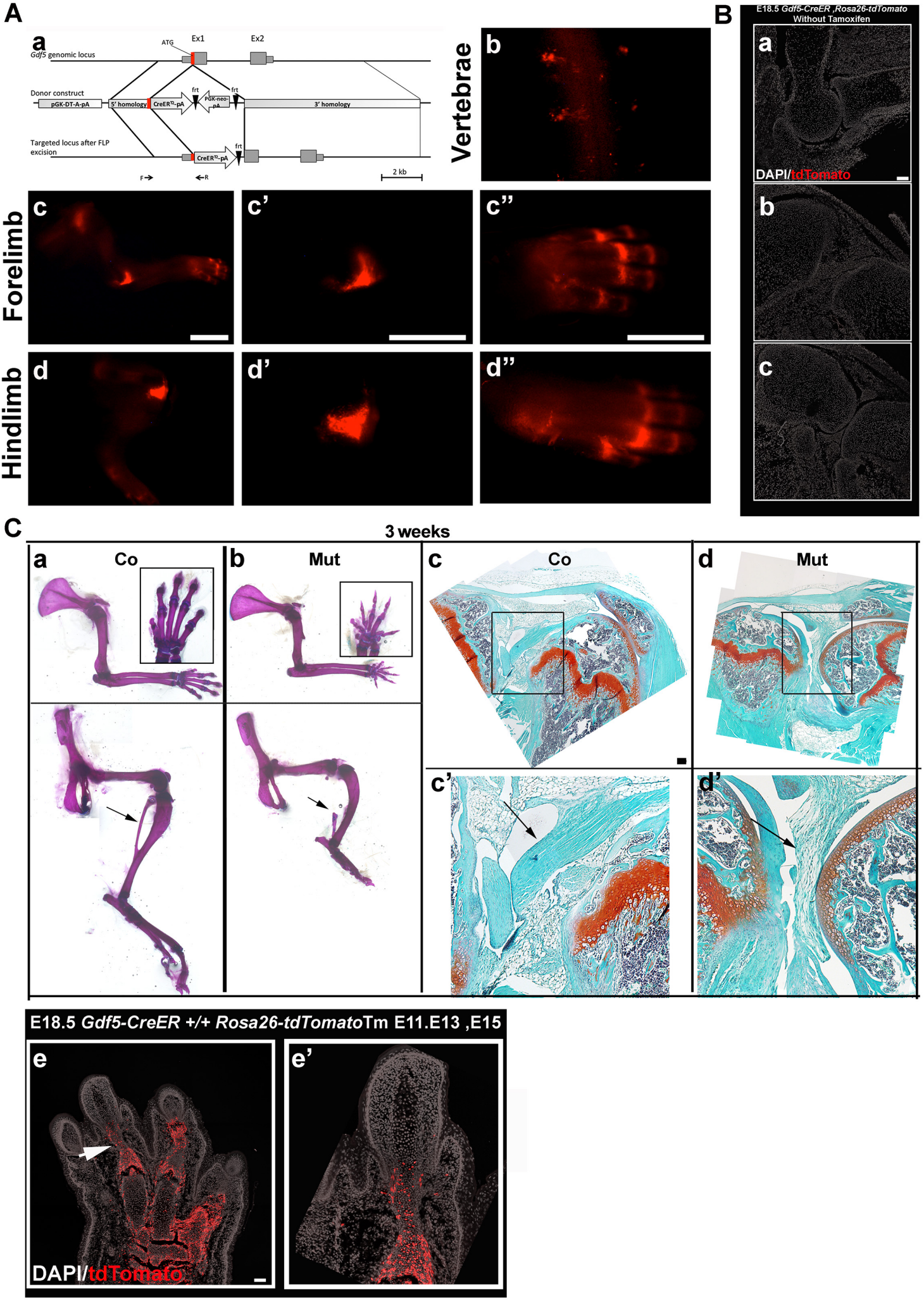
A
a
Gdf5 genomic locus
ATG
Ex1
Ex2
Donor construct
pGK-DT-A-pA
5' homology
CreER^T2-pA
frt
PGK-neo-pA
3' homology
Targeted locus after FLP excision
F
R
2 kb
Vertebrae
b
Forelimb
c
c'
c''
Hindlimb
d
d'
d''
B
E18.5 Gdf5-CreER ,Rosa26-tdTomato
Without Tamoxifen
a
DAPI/tdTomato
b
c
C
3 weeks
a
Co
b
Mut
c
Co
d
Mut
c'
d'
E18.5 Gdf5-CreER +/+ Rosa26-tdTomatoTm E11.E13 ,E15
e
DAPI/tdTomato
e'

Figure S1. Validation of the *Gdf5-CreER* model (related to Figure 1)

(A) Generation of a new knock-in *Gdf5-CreER* line. (a) Construct design. (b-d'') Lineage tracing experiment, using the *Rosa26-tdTomato* mouse as a reporter, demonstrates the effectiveness and accuracy of the newly developed *Gdf5-CreER* mouse line. Following tamoxifen administration at E13.5, whole-mount preparations from E18.5 embryos exhibit staining in the joints of the vertebrae (b) as well as in various joints of the forelimb (c-c'') and hindlimb (d-d''). Magnifications of the forelimb elbow (c') and autopod (c'') joints and of the hindlimb knee (d') and autopod (d'') joints are shown. **(B)** Lineage tracing analysis using *Gdf5-CreER* mouse crossed with *Rosa26-tdTomato* mouse as a reporter without tamoxifen administration. Examination at E18.5 shows no tdTomato-positive cells in the elbow (a) and knee (b-c) joints **(C)** Homozygous *Gdf5-CreER* mice recapitulate the *Gdf5*-null phenotype. (a,b) Skeletal preparations of forelimb (upper panel) and hindlimb (lower panel) from 3 weeks old control (a, Co) and *Gdf5-CreER* homozygous (b, Mut) mice show malformed autopods, malformed fibula and a tibia with an increased bend in the mutant. (c-d') Safranin O staining of sections through the knee joint shows the absence of cruciate ligaments in mutant mice (d) as compared to control mice (c). (c',d'): Magnifications of the boxed areas in c,d, respectively. (e,e') Lineage tracing analysis using *Gdf5-CreER* homozygous mutant crossed with *Rosa26-tdTomato* mouse as a reporter demonstrates the expansion of the *Gdf5* expression domain following multiple tamoxifen (Tm) administrations (at E11.5, E13.5 and E15.5). Examination at E18.5 showed tdTomato-positive cells occupying a greater area of the autopod, especially in the digits (white arrow). (e'): Magnification of the digit area indicated by an arrow in e. Scale bars represent 1 mm in A and 100 μm in B-C.

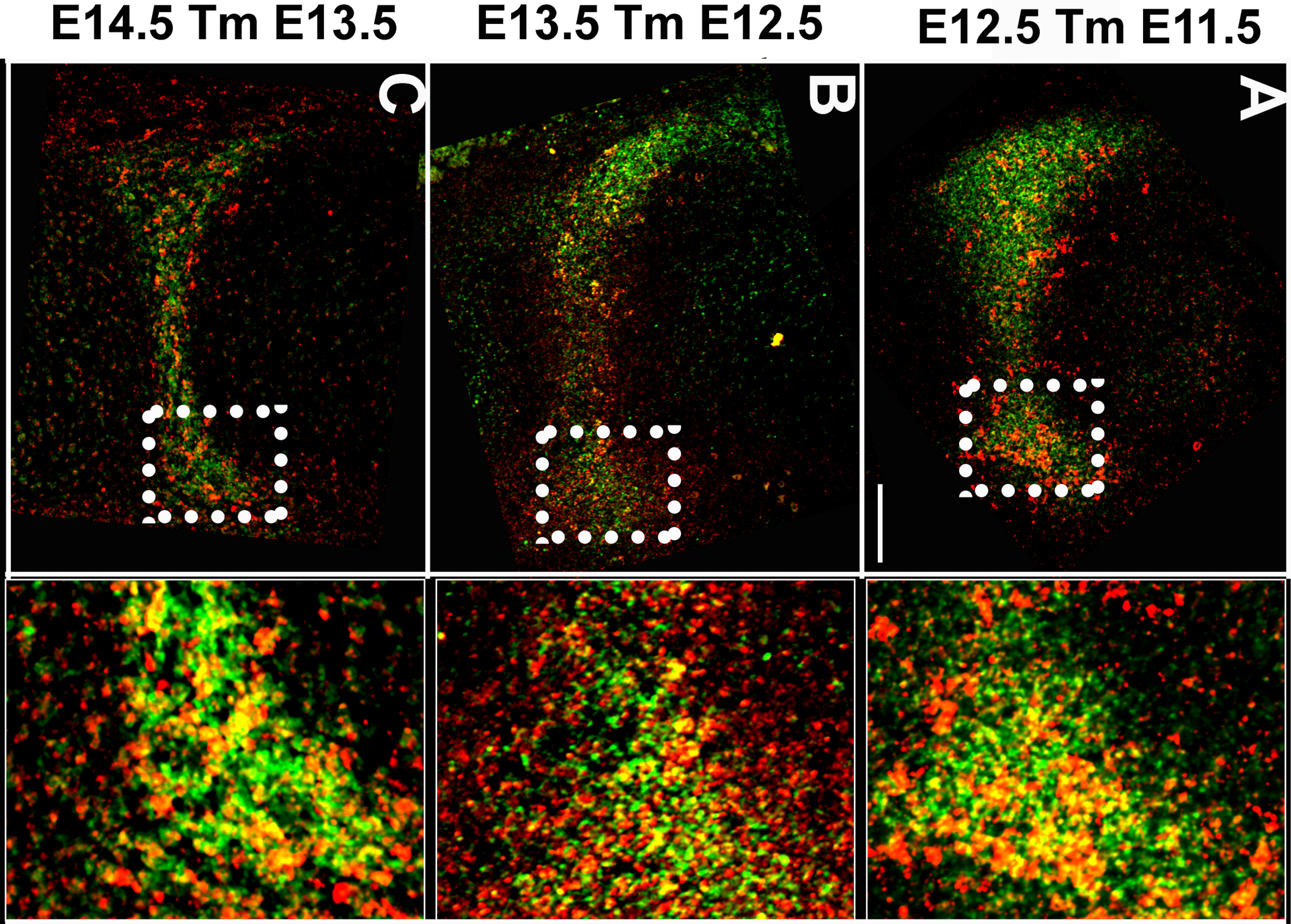
E14.5 Tm E13.5
E13.5 Tm E12.5
E12.5 Tm E11.5
C
B
A

Figure S2. Coexpression of *Gdf5* and *tdTomato* in the interzone (related to Figure 2)

(A-C) Double in situ hybridization for *Gdf5* (green) and *tdTomato* (red) genes at E12.5-E14.5, following administration of a single tamoxifen dose at E11.5-E13.5, respectively, shows high overlap between *Gdf5*- and *tdTomato*-expressing populations. Magnifications of the boxed areas are shown on the right. Scale bar represents 100 μm.

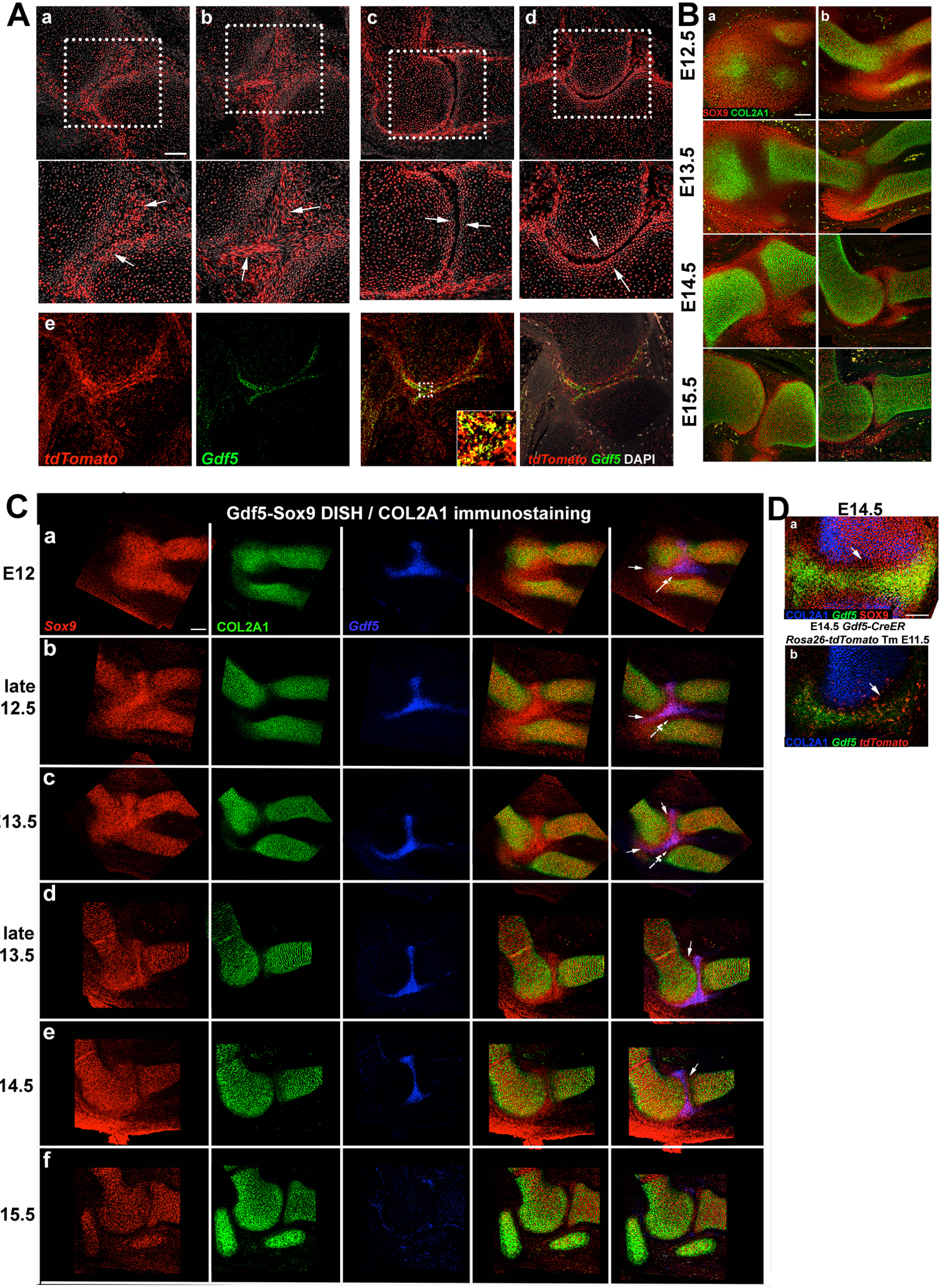
A
a
b
c
d
e
tdTomato
Gdf5
tdTomato Gdf5 DAPI
B
E12.5
E13.5
E14.5
E15.5
SOX9 COL2A1
C
Gdf5-Sox9 DISH / COL2A1 immunostaining
E12
late E12.5
E13.5
late E13.5
E14.5
E15.5
Sox9
COL2A1
Gdf5
D
E14.5
COL2A1 Gdf5 SOX9
E14.5 Gdf5-CreER
Rosa26-tdTomato Tm E11.5
COL2A1 Gdf5 tdTomato

Figure S3. Joint-forming cells originate from *Sox9*-positive cells (related to Figure 4)

(A) Pulse-chase lineage tracing experiment using *Sox9-CreER* mice crossed with *Rosa26-tdTomato* reporter mice shows that following a single tamoxifen administration at E10.5, all joint lineages are derived from early *Sox9*-expressing cells. **(a,b)** Sections through E15.5 knee. **(c,d)** Sections through E15.5 elbow joint. **(e)** Double in situ hybridization for *tdTomato* and *Gdf5*. **(B)** Immunofluorescent staining for SOX9 and COL2A1 on sections through E12.5-E15.5 knee (a) and elbow (b) joints**. (C)** *Gdf5* and *Sox9* double ISH and COL2A1 immunofluorescent staining on sections through E12-E15.5 elbow (a-f) joints. Arrows indicate a population of *Sox9*-positive *Gdf5*, COL2A1-negative cells outside (arrows) and inside (dashed arrows) the interzone. **(D**) Analysis of *Gdf5* gene expression (green) and double immunofluorescent staining for COL2A1 (blue) and SOX9 (red) on section through the knee joint at E14.5. **(a)** In wild-type mice, an intra-articular population of SOX9-positive, *Gdf5*, COL2A1-negative cells is indicated by an arrow. **(b)** Pulse-chase experiment using *Gdf5-CreER* mice crossed with *Rosa26-tdTomato* reporter mice. Following tamoxifen (Tm) administration at E11.5, the area corresponding to the intra-articular SOX9-positive, *Gdf5*, COL2A1-negative population (arrow) is occupied by cells expressing *tdTomato* but not *Gdf5*. Scale bar represents 100 μm.

Supplemental Experimental Procedures

Animals

To generate *Gdf5-CreER* knock-in mouse, a targeting vector (donor construct) was designed to introduce *Cre-ER*^{T2} fusion gene and an FRT-flanked neo cassette at the ATG of the *Gdf5* locus. The construct was electroporated into embryonic stem (ES) cells. PGK-diphtheria toxin cassette was used in the construct to ensure survival of correctly targeted clones only, which would lose the diphtheria toxin due to correct homologous recombination event. ES cells were then injected into recipient blastocysts and chimeric mice were bred with flippase transgenic mice to delete the neo cassette and produce mice that were used to generate a *Gdf5-CreER*-positive colony. In Figure 1A, arrows indicate the location of the forward and reverse primers used to verify correct targeting of the *Gdf5* locus.

Sox9-CreER^{T2} mice were previously described (Soeda et al., 2010).

Tamoxifen administration

For lineage tracing analysis, pregnant female *Sox9-CreER* mice were administered 0.3 mg/g tamoxifen/body weight in corn oil by oral gavage.

Histological analysis

For paraffin sectioning, embryos were fixed overnight in 4% PFA/PBS, dehydrated to 100% EtOH, embedded in paraffin and sectioned at a thickness of 7 μm. Safranin O staining was performed according to the standard protocol.

Immunofluorescent staining

For paraffin section immunofluorescence, embryos were fixed overnight in 4% PFA/PBS, dehydrated to 100% EtOH, embedded in paraffin and sectioned at a thickness of 7 μm. 10 mM sodium citrate (pH 6.0) was used for antigen retrieval. Slides were incubated overnight at 4°C with primary antibody anti-SOX9 (EMD Millipore) 1:150 in blocking solution. Then, slides were subjected to additional digestion by Proteinase K (sigma) and incubated overnight at 4°C with primary antibody anti-COL2 ((DSHB) 1:50 in blocking solution. Following fluorescence in situ hybridization, slides were incubated overnight at 4°C with primary antibody anti-COL2 (1:50) and anti-SOX9 (1:150) in blocking solution.

Skeletal preparations

Cartilage and bones in whole mouse embryos were visualized after staining with Alcian blue and Alizarin red S (Sigma) and clarification of soft tissue with potassium hydroxide (McLeod, 1980).

In situ hybridization

For double ISH: after hybridization, slides were washed, quenched and blocked. Probes were detected by incubation with anti-fluorescein-POD and anti-DIG-POD (Roche; 1:200), followed by Cy3-, Cy2- or Cy5-tyramide labeled fluorescent dyes (according to the instructions of the TSA Plus Fluorescent Systems Kit, Perkin Elmer). *tdTomato* antisense probe was generated using the following primers: Forward, tcccacaacgaggactacaccat, reverse, cgcgcatcttcaccttgtagatca.

Co-localization measurements

Masking was performed using the *Gdf5* channel prior to automatic thresholding (Costes method) for both channels. For *Gdf5* and *tdTomato* co-localization, the value of "% of material *Gdf5* above threshold colocalized" was used. For the prevalence of *tdTomato*-positive, *Gdf5*-negative cells, the value "100%-% of material *tdTomato* above threshold colocalized" was used.

Supplemental References

McLeod, M.J. (1980). Differential staining of cartilage and bone in whole mouse fetuses by alcian blue and alizarin red S. Teratology *22*, 299-301.